https://doi.org/10.37434/tpwj2021.01.06

# NUMERICAL ANALYSIS OF THE FEATURES OF LIMITING STATE OF WELDED PIPELINE ELEMENTS UNDER ULTRA-LOW-CYCLE LOADING CONDITIONS

**O.V. Makhnenko, O.S. Milenin, O.A. Velykoivanenko, G.P. Rozynka** and **N.I. Pivtorak**
E.O. Paton Electric Welding Institute of the NAS of Ukraine
11 Kazymyr Malevych Str., 03150, Kyiv, Ukraine. E-mail: office@paton.kiev.ua

Expert analysis of the reliability and performance of welded pipelines with detected corrosion-erosion damage under ultra-low-cycle loading requires taking into account several interrelated physicomechanical phenomena, which determine the limiting state of a specific structure. For this purpose, integrated numerical procedure was developed in this study for finite-element assessment of subcritical fracture accumulation and prediction of the limiting state of typical pipelines with 3D defects of wall thinning. The ductile mechanism of subcritical fracture was considered as the main one. Moreover, material hardening and softening at plastic deformation (strain hardening, Bauschinger effect) was taken into account. This integrated approach allowed revealing the main regularities of failure of a typical pipeline element, depending on external loading. 14 Ref., 7 Figures.

*Keywords: welded pipeline, corrosion-erosion defect, ultra-low-cycle loading, Bauschinger effect, ductile fracture, limiting state*

Numerical assessment of residual strength of pipeline elements (PE) with detected corrosion-erosion losses of metal is a characteristic problem at expert analysis of the reliability of various industrial systems. A generally accepted approach to solution of this problem is evaluation of the limiting state of a specific structure at nominal service load. As the majority of pipelines are welded, the impact of the residual stress-strain state (SSS) should be taken into account, if metal losses are in the welding zone. This problem is well studied for static loading (for instance, by internal pressure) [1–3], whereas for cyclic force impact the spatial inhomogeneity and interrelation of physicomechanical processes, which cause subcritical damage and failure of material, require a considerable conservatism of the respective analytical methods. In particular, ultra-low-cycle fatigue differs by considerable plastic flow of the material that requires taking into account its strain hardening, softening by Bauschinger effect and initiation of ductile fracture pores [4]. Presence of the welded joint and local geometrical anomalies of the structure (service defects of corrosion-erosion loss of metal) determines the features of the stress-strain state of pipeline elements under the impact of internal pressure and/or bending moment and influences the fracture resistance.

In this work the characteristic features of subcritical damage accumulation and limiting state of welded pipelines with corrosion-erosion metal loss at ultra-low-cycle loading were studied on the base of finite-element prediction.

**Mathematical model of the kinetics of welded PE state under the impact of static and cyclic loading**. Limiting state of corroded (eroded) PE depends on a range of physicomechanical processes, initiated by operational and technology impact. In the case of a significant deformation under cyclic loading (for instance, earthquake, landslide, overload, stability loss, etc.) the limiting state of the pipeline is determined by development of plastic strains and respective accumulation of subcritical damage right up to initiation of a macrodefect. Local metal losses and respective mechanical stress raisers lead to a certain lowering of PE load-carrying capacity under pressure. Their admissibility is determined by the respective standard norms for design operation conditions. However, ultra-low-cycle loading (number of cycles from 10 to 100) leads to extraordinary modes of pipeline operation that complicates expert analysis of their compliance with design requirements. The main complexity consists in the nonlinear reaction of the material to cyclic plastic deformation and development of its properties. Thus, alongside the characteristic strain hardening two possible mechanisms of material softening can be singled out: Bauschinger effect due to a change in plastic strain direction and accumulation of ductile fracture porosity with concurrent reduction of the load-carrying net cross-section of the structure [5]. Presence of welds causes spatial heterogeneity of

O.V. Makhnenko — https://orcid.org/0000-0002-8583-0163, O.S. Milenin — https://orcid.org/0000-0002-9465-7710

SSS and complex interaction of operational and residual stresses. This should be also taken into account, particularly in the case of close proximity of metal loss area and weld.

In the absence of sharp-angled geometrical stress raisers, the prevailing mechanism of violation of material integrity is ductile failure, which consists in initiation of uniformly distributed pores [6]. In order to predict their initiation at plastic flow of material in nonisothermal cases, it is proposed to use the deformation criterion, in keeping with which initial porosity with bulk concentration $f_0$ appears in a certain volume of metal at fulfillment of the following condition:

$$\int \frac{d\varepsilon_i^p}{\varepsilon_c(T)} > 1, \quad (1)$$

where $d\varepsilon_i^p = \sqrt{2}/3\sqrt{d\varepsilon_{ij}^p d\varepsilon_{ij}^p}$ is the intensity of plastic strain increment; $\varepsilon_c(T)$ is the critical value of plastic strains; $i, j = r, \beta, z$ are the coordinates in the cylindrical system of coordinates (Figure 1).

Further increase of the concentration of ductile fracture pores during plastic deformation of metal, in particular, at static or cyclic loading in service, corresponds to Rice–Tracey law [7]:

$$df = \begin{cases} 1.28\exp\left(\frac{3}{2}\frac{\sigma}{\sigma_i}\right)d\varepsilon_i^p, \text{ if } \frac{\sigma}{\sigma_i} > 1 \\ 1.28\left(\frac{\sigma}{\sigma_i}\right)^{1/4}\exp\left(\frac{3}{2}\frac{\sigma}{\sigma_i}\right)d\varepsilon_i^p, \text{ if } \frac{1}{3} \le \frac{\sigma}{\sigma_i} \le 1 \end{cases}, \quad (2)$$

Mathematical treatment of the joint problem of temperature field kinetics in welding, SSS development and micropore formation is based on finite-element description using eight-node finite elements (FE). Increment of strain tensor was presented as a sum of the respective components [8]:

$$d\varepsilon_{ij} = d\varepsilon_{ij}^e + d\varepsilon_{ij}^p + \delta_{ij}\left(d\varepsilon_T + df/3\right), \quad (3)$$

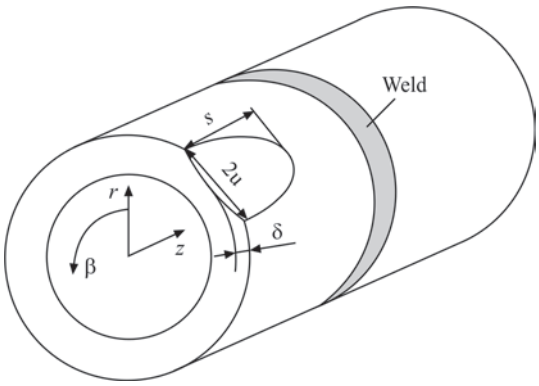


**Figure 1.** Scheme of a section of defective pipeline in the cylindrical system of coordinates

where $d\varepsilon_{ij}^e$, $d\varepsilon_{ij}^p$, $\delta_{ij}d\varepsilon_T$, $\delta_{ij}df/3$ are the components of increment of strain tensor due to elastic deformation mechanism, deformations of instantaneous plasticity, kinetics of heterogeneous temperature field and porosity, respectively.

Proceeding from the above-said, the strain tensor increments can be represented in the form of superposition of increments of the respective components:

$$\Delta\varepsilon_{ij} = \Psi\left(\sigma_{ij} - \delta_{ij}\sigma\right) + \delta_{ij}\left(K\sigma + \Delta\varepsilon_T + \Delta f/3\right) - \frac{1}{2G}\left(\sigma_{ij} - \delta_{ij}\sigma\right)^* - \left(K\sigma\right)^*, \quad (4)$$

where «*» symbol refers the respective variable to the previous tracing step; $\Psi$ is the material state function, which determines the plastic flow conditions according to Mises criterion, additionally taking into account the reduction of the load-carrying net cross-section of the finite element as a result of discontinuity formation within Gurson–Tvergaarten–Needleman model [9]:

$$\Psi = \frac{1}{2G}, \text{ if } \sigma_i < \sigma_s = \sigma_y\sqrt{1 + \left(q_3 f'\right)^2 - 2q_1 f'\cosh\left(q_2\frac{3\sigma}{2\sigma_y}\right)}, \quad \Psi > \frac{1}{2G}, \text{ if } \sigma_i = \sigma_s, \quad \text{state } \sigma_i > \sigma_s \text{ is invalid.} \quad (5)$$

Determination of $\Psi$ function is performed by iteration at each step of numerical tracing (by time or load increment) within the finite-element solution of the boundary problem of nonstationary thermoplasticity that allows solving the nonlinearity problem by the material plastic flow, allowing for its subcritical damage [10]. The main difficulty in modeling the cyclic loading consists in that small changes in the state of metal in one loading cycle, namely accumulation and increase of subcritical damage, cause a change in the yield surface and a respective change of plastic deformation loop. However, at each loading step it is necessary to determine the equilibrium state of damage and the respective distribution of stresses and strains. For this purpose, proceeding for the assumption that the stationary state is characterized by a negligibly small rate of increase of ductile fracture pore volume, it is proposed to conduct the following iteration process by $\Psi_k$ function:

$$F = \begin{cases} F + dF, \text{ if } f_0 K_1 \exp\left(K_2\frac{\sigma}{\sigma_i}\right)d\varepsilon_i^P = \\ = \Psi_k \le \Psi_k^0 \approx 10^{-5}; \\ F, \text{ if } \Psi_k > \Psi_k^0, \end{cases} \quad (6)$$

where $F$ is the system of external force loads acting on the structure; d$F$ is the increment of force loads during numerical tracing; $K_1$, $K_2$ are the constants.

Strain hardening of the metal affects the shape of Mises yield surface, which, depending on the intensity of the accumulated plastic strains, is usually considered in the following form [11]:

$$\sigma_T = \sigma_T^0 \left[ 1 + c_1 \ln\left( \frac{\dot{\varepsilon}^p}{\dot{\varepsilon}_0} \right) + c_2 \left\{ \ln\left( \frac{\dot{\varepsilon}^p}{\dot{\varepsilon}_0} \right) \right\}^2 \right] \times \times \left[ 1 + \left( \frac{\varepsilon^p}{\varepsilon_0} \right) \right]^m, \quad (7)$$

where $c_1 = 2.149 \cdot 10^{-3}$; $c_2 = 9.112 \cdot 10^{-2}$; $\varepsilon_0 = 1.540 \cdot 10^{-4}$, $m = 0.14$ are the constants; dot above a variable denotes time differentiation.

If it is necessary to take into account the change of plastic deformation direction (for instance, at variable static loading that causes an alternating cycle of plastic deformation), a model of kinetic strengthening of the material was used in the following form [12]:

$$\sqrt{\frac{3}{2}\left(\sigma_{ij} - \delta_{ij}\sigma - \overline{X}\right)\left(\sigma_{ij} - \delta_{ij}\sigma - \overline{X}\right)} - \\ -\sigma_T'(f')\left[1 + \left(\varepsilon^p / \varepsilon_0\right)\right]^M \le 0, \quad (8)$$

where $\sigma_T'(f')$ is the current true yield strength of the damaged material in keeping with (9); $M$, $\varepsilon_0$ are the material constants; $\overline{X}$ is the shear tensor:

$$\overline{X} = \operatorname{sign}\left(\varepsilon^p\right)\frac{C}{\gamma} + \left[ X_0 - \operatorname{sign}\left(\varepsilon^p\right)\frac{C}{\gamma} \right] \times \\ \times \exp\left[ -\operatorname{sign}\left(\varepsilon^p\right)\left(\varepsilon^p - \varepsilon_0^p\right) \right]. \quad (9)$$

Proceeding from a specific value of $\Psi$ function, the strain field at each loading stage is determined from (5), taking into account $\sigma_s(T, \varepsilon^p)$ dependence. The components of stress tensor satisfy the statics equation for internal FE and boundary conditions for surface FE. In their turn, the components of $\Delta U_i = (\Delta U, \Delta V, \Delta W)$ vector satisfy the respective conditions on the boundary. The solved system of equations in variables of the vector of displacement increments in FE nodes is determined at each step of tracing and iterations by $\Psi(\Psi_k)$ by minimizing the following functional [13]:

$$E_l = -\frac{1}{2}\sum_V \left(\sigma_{ij} + J_{ij}\right)\Delta\varepsilon_{ij} V_{m,n,r} + \\ + \sum_{S_P} F_i \Delta U_i \Delta S_P^{m,n,r}, \quad (10)$$

where $\sum_V$ is the operator of the sum of inner FE; $\sum_{S_P}$ is the operator of the sum of surface FE, on which the components of force vector $F_i$ are assigned.

A criterion for initiation of macrodefectiveness of PE material, is fulfillment of one of the three fracture conditions [14]:

$$\Psi \ge \frac{1}{2G} + \frac{\varepsilon_f - \left(\varepsilon_i^p\right)^*}{1.5\sigma_s\left(\varepsilon_i^p\right)}; \\ f' \ge f_F = \frac{1}{q_1}\exp\left( -\frac{3q_2\sigma_m}{2\sigma_Y} \right); \quad (11) \\ \frac{\sigma_1}{1 - 2f/3} > S_K,$$

where $\varepsilon_f$ is the ultimate strain which, in the general case, depends on the stressed state rigidity; $S_K$ is the microcleavage stress; $q_1$, $q_2$ are the constants.

If the above-mentioned process of loss of FE load-carrying capacity proceeds at this loading stage, covering an ever greater number of neighbouring FE, and does not allow moving to the next loading step then this step determines the boundary loading of «spontaneous failure».

**Results and discussion.** As was noted above, residual SSS in the weld area, kinematic hardening and ductile fracture affect the limiting state of the effective PE at ultra-low-cycle loading by internal pressure and bending moment. One of the main problems, which were to be solved using the developed numerical approach, is determination of the influence of these interrelated phenomena on the load-carrying capacity of a specific welded structure. Considered for this purpose, was a characteristic example of PE of $D \times t$ = 315×10 mm size from stainless steel 316L ($E$ = 193 GPa, $\nu$ = 0.3, $\sigma_T$ = 170 MPa) with local erosion loss of metal of a semi-elliptical shape on the pipe inner surface ($2s \times 2u \times \delta$ = 40×20×5 mm). Examples of stress distribution over the pipe cross-section after welding and under the working conditions are given in Figure 2.

Figure 3, *a* shows the dependencies of local stresses $\sigma_{\beta\beta}$ on strain $\varepsilon_{\beta\beta}$ near the internal defect of erosion thinning, taking and not taking into account plastic damage of the material caused by internal pressure $P$ = 10 MPa and bending moment $M$ from –85 to 85 kN (that corresponds to the range of maximum axial stress range from –120 to 120 MPa). As one can see, accumulation of ductile fracture porosity at plastic deformation of the steel pipe leads to displacement of stress hysteresis loops to higher strains through softening of porous materials and reduction of the load-carrying structure cross-section.

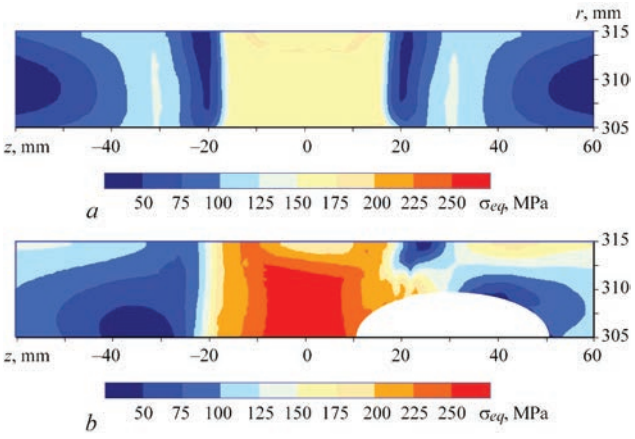


**Figure 2.** Calculated distributions of intensity of stresses $\sigma_i$ in the pipeline ($D \times t$ = 315×10 mm, 316L stainless steel): *a* — residual state in the area of a circumferential site weld; *b* — with internal erosion defect ($2s \times 2u \times \delta$ = 40×20×5 mm) at working pressure $P$ = = 8.0 MPa

The intensity of plastic damage accumulation at ultra-low-cycle loading (i.e the rate of increase of porosity volume concentration $f$ per cycle number $N$) has three main stages: plastic strain prior to plastic damage initiation; porosity initiation and redistribution of strain and stress fields; stable increase of plastic strains and concentration of porosity volume up to the limiting state. The first two stages correspond to static loading and proceed in the first cycles, while the third stage is related to fatigue fracture of plastically deformed material. Figure 3, *b* shows the results of numerical evaluation of plastic damage accumulation for the considered case of eroded PE at the stable growth stage. As one can see, porosity concentration $f$ rises quasilinearly, starting from the second loading cycle by the bending moment at the same internal pressure $P$. It means that increase rate $f$ depends mainly on the

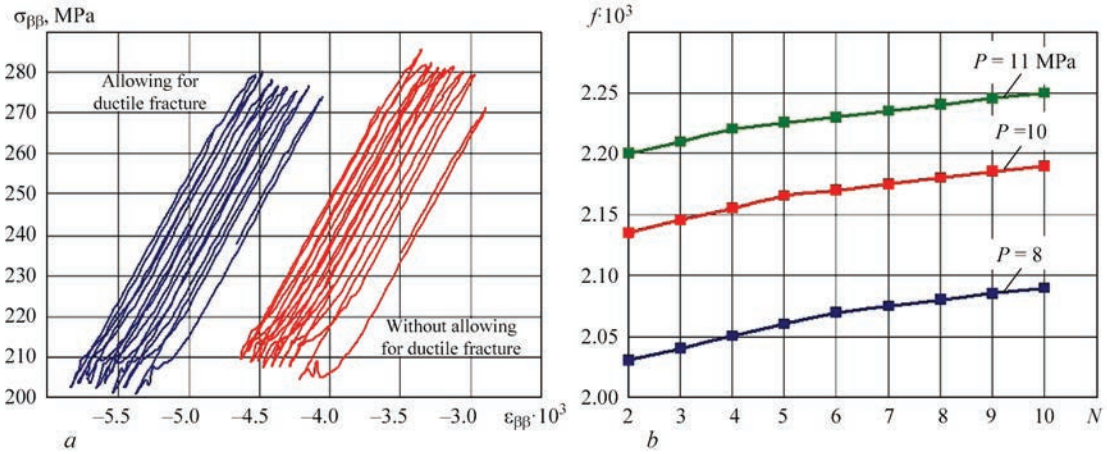


**Figure 3.** Dependencies of stresses $\sigma_{\beta\beta}$ on stains $\varepsilon_{\beta\beta}$ near an internal defect of erosion wall thinning ($2s \times 2u \times \delta$ = 40×20×5 mm) of pipeline element ($D \times t$ = 315×10 mm, 316L stainless steel), taking and not taking into account the material damage by the ductile mechanism (internal pressure $P$ = 10 MPa and bending moment $M$ = –85–85 kN·m) (*a*) and of maximum volume concentration of pores $f$ on cycle number $N$ (*b*)

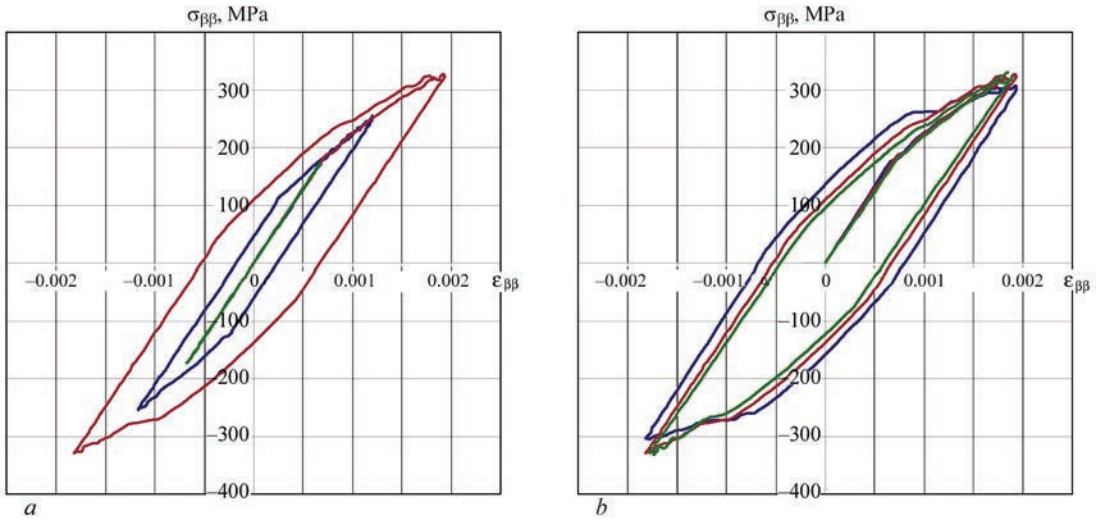


**Figure 4.** Impact of alternating internal pressure on the kinetics of stress-strain state of defective welded PE ($D \times t$ = 315×10 mm, 316L stainless steel): (*a*) — $2s \times 2u \times \delta$ = 40×20×5 mm, $P$ = –20÷20 MPa, $M$ = 0 kN·m (●), $P$ = –30–30 MPa, $M$ = 0 kN·m (▲), $P$ = = –40–40 MPa, $M$ = 0 kN·m (■); (*b*) — $P$ = –40–40 MPa, $M$ = 0 kN·m, $2s \times 2u \times \delta$ = 40×20×4 mm (●), $2s \times 2u \times \delta$ = 40×20×5 mm (■), $2s \times 2u \times \delta$ = 40×20×6 mm (▲)

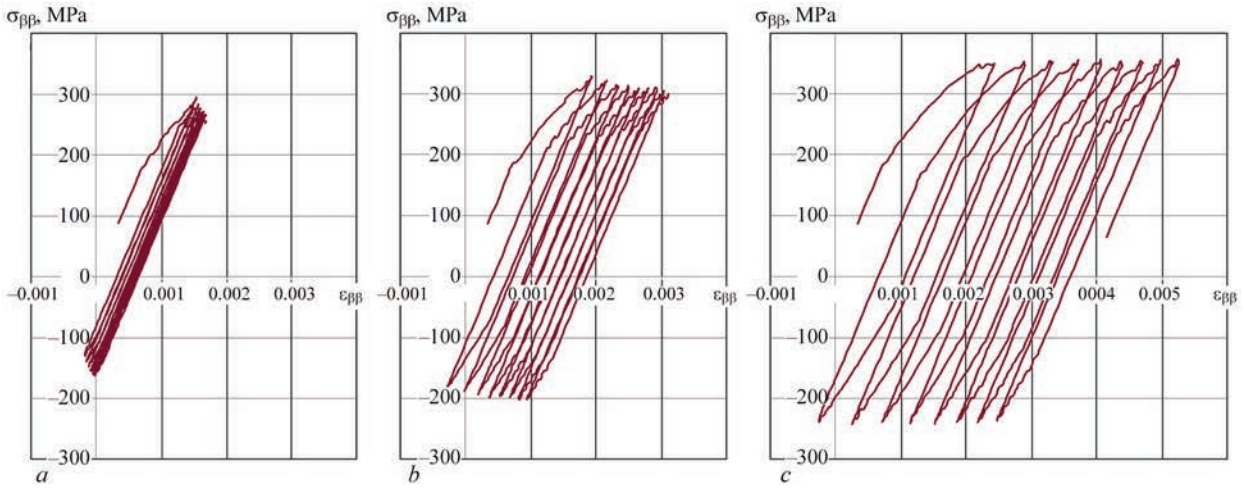


**Figure 5.** Features of the impact of asymmetry of the cycle of PE ((*D*×*t* = 315×10 mm, 316L stainless steel) loading by internal pressure on the kinetics of plastic strain accumulation: *a* — *P* = –15–35 MPa, *M* = 0 kN·m; *b* — *P* = –20–40 MPa, *M* = 0 kN·m; *c* — *P* = = –25–45 MPa, *M* = 0 kN·m

applied range of bending loading, and not on the path of plastic (or general) deformation.

It should be noted that in the case of impact of solely pressure varying by a symmetrical cycle (for instance, in the case of underwater pipelines or complex pressure vessels – carrier rocket tanks, exposed to both internal and external pressure), the dependence of current stresses on strains in the characteristic area of stress raiser of PE with wall thinning defect, has the classical form of a closed hysteresis loop (Figure 4). The size and shape of the loop in such a case depend on the range of pressure values, as well as on the defect size. It means that performance limitation in such a case is due solely to accumulation of subcritical damage by the ductile mechanism, which causes gradual destruction of the material and it reaching the limiting state. At loading cycle asymmetry, the intensities of the positive and negative plastic strains are not balanced that causes gradual displacement of the hysteresis loop along the strain axis (Figure 5). For the mentioned case it is attributable for greater influence of strain hardening, compared to Bauschinger effect.

For practically important cases, such an asymmetry of the cycle is characteristic of pipelines under pressure, which are additionally cyclically loaded by an alternating bending moment. Here, a constant component, which is proportional to internal pressure, is added to bending longitudinal stresses and strains proper, which typically change by a symmetrical cycle, in keeping with the solution of Lame problem. Therefore, it is to be expected that at unchanged cycle of loading by bending moment, increase of internal pressure will have a significant negative impact on the load-carrying capacity of a defective pipeline for the reason of a considerable displacement of the hysteresis loop of the stress-strain state. This is confirmed by calculation results given in Figure 6.

A characteristic feature of the field of bulk concentration of subcritical damage *f* in the cross-section of a defective pipeline, that is under the impact of both

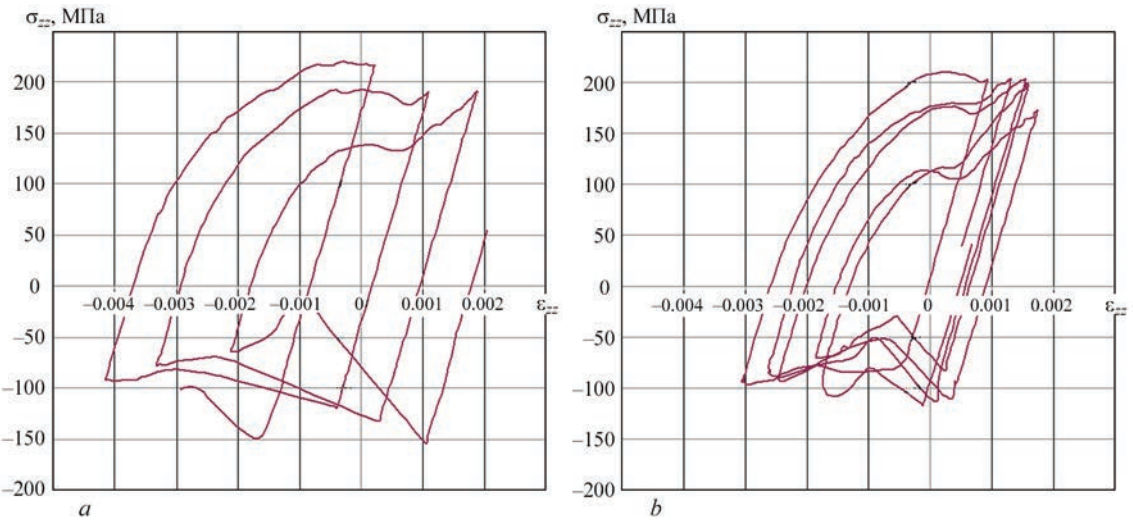


**Figure 6.** Kinetics of stress-strain state of defective welded PE ((*D*×*t* = 315×10 mm, 316L stainless steel) under the impact of cyclic loading by bending moment: *a* — *P* = 10 MPa, *M* = –70–70 kN·m; *b* — *P* = 8 MPa, *M* = –70–70 kN·m

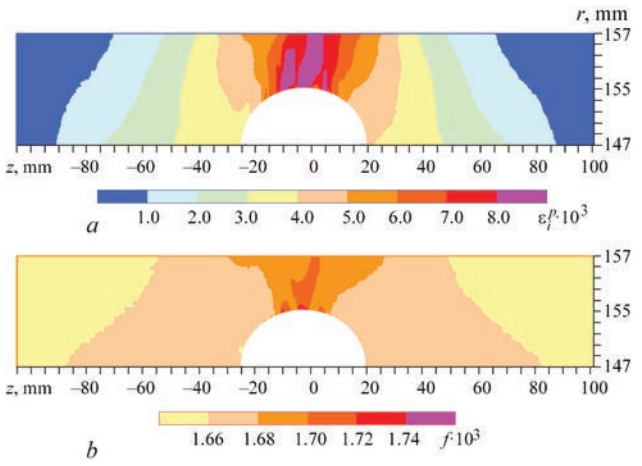


**Figure 7.** Distribution of plastic strain intensity (*a*) and concentration of ductile fracture pores (*b*) in the cross-section of pipeline element ($D \times t$ = 315×10 mm, 316L stainless steel) with internal wall thinning ($2s \times 2u \times \delta$ = 40×20×5 mm) in the limiting state at internal pressure $P$ = 8 MPa and cyclic bending moment $M$ = = –85–85 kN·m)

internal pressure and alternating bending moment, is a sufficiently narrow area of maximum pore concentration in the current and limiting state of the structure (Figure 7). This is attributable to the fact that depending on deformation direction under cyclic loading conditions, the maximum and minimum stresses form alternatively on different surfaces of the pipe in the geometrical stress raiser area.

## Conclusions

1. Mathematical models of the stress-strain and damage state of pipeline elements with detected defects of local wall thinning at ultra-low-cycle loading were constructed. In order to adequately take into account the nonlinearity of material properties at cyclic plastic deformation (Bauschinger effect) and ductile fracture accumulation, an appropriate description of the surface of plastic flow of the material within the conceptual model of elasto-plastic continuum was proposed.

2. A characteristic example of a welded pipeline element ($D \times t$=315×10 mm, 316L stainless steel) with detected internal defect of erosion thinning of the wall was used to show the features of stress-strain kinetics under the conditions of loading by cyclic internal pressure and bending moment. An essential impact of loading cycle asymmetry on plastic damage accumulation is shown: violation of the balance between strain hardening and softening by Bauschinger effect causes a gradual displacement of the stress-strain state loop.

3. It is shown that accumulation of plastic strains during alternating cyclic loading causes initiation and growth of ductile fracture pores in the area of a defect of local wall thinning with formation of a rather narrow area of maximum pore concentration. This is caused by the fact that under the conditions of cyclic loading the maximum and minimum stresses form at different surfaces of the pipe in the area of the geometrical stress raiser (depending on the cycle).


1. (2004) *Recommended practice*, DNV-RP-F101. Corroded Pipelines. Ed. by O. Bjornoy. Hovik, Det Norske Veritas..
2. Hertelé, S., Cosham, A., Roovers, P. (2016) Structural integrity of corroded girth welds in vintage steel pipelines. *Engineering Structures*, **124**, 429–441. DOI: https://doi.org/10.1016/j.engstruct.2016.06.045
3. Milenin, A., Velikoivanenko, E., Rozynka, G., Pivtorak, N. (2019) Probabilistic procedure for numerical assessment of corroded pipeline strength and operability. *Int. J. of Pressure Vessels and Piping*, **171**, 60–68. DOI: https://doi.org/10.1016/j.ijpvp.2019.02.003
4. Morin, L., Michel, J.-C., Leblond, J.-B. (2017) A Gurson-type layer model for ductile porous solids with isotropic and kinematic hardening. *Int. J. of Solids and Structures*, **118–119**, July, 167–178. https://doi.org/10.1016/j.ijsolstr.2017.03.028
5. Chun, B.K., Jinn, J.T., Lee, J.K. (2002) Modeling the Bauschinger effect for sheet metals, Pt I: Theory. *Int. J. of Plasticity*, **18**, 571–595. DOI: https://doi.org/10.1016/S0749-6419(01)00046-8
6. Xue, L. (2008) Constitutive modeling of void shearing effect in ductile fracture of porous materials. *Engineering Fracture Mechanics*, **75**, 3343–3366. DOI: https://doi.org/10.1016/j.engfracmech.2007.07.022
7. Chen, Z., Butcher, C. (2013) *Micromechanics Modelling of Ductile Fracture*. Dordrecht, Springer Netherlands. https://doi.org/10.1007/978-94-007-6098-1
8. Makhnenko, V. (2013) Problems of examination of modern critical welded structures. *The Paton Welding J.*, **5**, 21–28.
9. Zhang, Z.L. (2001) *A complete Gurson model.* Nonlinear fracture and damage mechanics. Ed. by M.H. Alibadi. UK, WIT Press Southampton, 223–248.
10. Velikoivanenko, E., Milenin, A., Popov, A. et al. (2019) Methods of numerical forecasting of the working performance of welded structures on computers of hybrid architecture. *Cybernetics and Systems Analysis*, 55(**1**), 117–127. DOI:https://doi.org/10.1007/s10559-019-00117-8
11. Cowper, G.R., Symonds, P.S. (1958) *Strain hardening and strain rate effects in the impact loading of cantilever beams*. Brown Univ., Applied Mathematics Report.
12. Lemaitre, J., Chaboche, J.-L. (1990) *Mechanics of solid materials.* Cambridge, Cambridge University Press. https://doi.org/10.1017/CBO9781139167970
13. Makhnenko, V.I. (2006) *Safe service life of welded joints and assemblies of modern structures.* Kiev, Naukova Dumka [in Russian].
14. Milenin, O. (2017) Numerical prediction of the current and limiting states of pipelines with detected flaws of corrosion wall thinning. *J. of Hydrocarbon Power Engineering*, 4(**1**), 26–37.


Received 30.11.2021